T-REX: Numerical tool for tungsten damage assessment for DEMO

Alan Durif, Marianne Richou, Jean-Michel Bergheau, Laurent Gallais, Guillaume Kermouche, Gerald Pintsuk

T-REX: numerical tool for tungsten damage assessment for DEMO

A. DURIF[a,*], M. RICHOU[a,], J-M. BERGHEAU[b], L.GALLAIS[c], G.KERMOUCHE[d], G.PINTSUK[e]

[a] CEA, IRFM, F-13108 Saint-Paul-Lez-Durance, France
[b] University of Lyon, Ecole Centrale de Lyon, LTDS, CNRS UMR 5513, 42023 Saint-Etienne, France
[c] Aix Marseille Univ, CNRS, Centrale Marseille, Institut Fresnel, Marseille, France
[d] Mines Saint-Etienne, CNRS, UMR 5307 LGF, Centre SMS, F – 42023 Saint-Etienne, France
[e] Forschungszentrum Jülich GmbH, Institut für Energie- und Klimaforschung – Plasmaphysik, 52425, Jülich, Germany

Abstract

One of the R&D focus in the European fusion energy program is to establish a physical and technological basis for reliable power exhaust during entire operational situations of a DEMOstrational power plant. Following the design adopted for ITER, the baseline Plasma Facing Component for DEMO divertor is made of tungsten as armor material. The tungsten divertor target are the most thermally loaded in-vessel components in fusion reactor. The PFCs lifetime is affected by material degradations under the different loadings including High Heat Flux (HHF) and neutron irradiation. It has been reported a loss of mechanical properties due to softening (restoration/recrystallization). Latest finite element modeling developments allow to estimate component lifetime under HHF loading taking into account the progressive mechanical properties change due to softening. We propose here to take into account the influence of thermal and neutron loadings on the tungsten mechanical properties change for PFC lifetime assessment. For this, up to date mechanical properties of tungsten, softened tungsten, and neutron-irradiated tungsten are used as input data in the tool named T-REX (for Tungsten-Response based on EXperimental data). This tool is implemented as a user subroutine in a finite elements code. The influence of the neutron irradiation is studied as function of the dpa dose, the incident heat flux intensity and the current defined divertor component geometries (ITER and DEMO). With the study performed, it is shown that the geometry may be optimized to reduce the damage induced by plasticity. The numerical results also highlights that the plastic strain increment obtained after each thermal cycle reduces with the dpa dose.

Keywords: DEMO, tungsten, modeling, lifetime, damage, softening, irradiation, neutron

1. Introduction

In tokamak, magnetic confinement is imperfect [1, 2]. In WEST and ITER, the magnetic configuration drives the charged particles losses (including thermal heat flux loading) toward the main wall, mainly on the divertor target region where active pumping allows gas recycling and He/alpha particles exhaust [3]. In this context, the divertor components are the components which are the most thermally exposed. This thermal load results in particular from the particles bombardment (ions, electrons, neutrals) coming from the plasma, the radiation, the energy conducted along the magnetic lines and from neutron irradiation. The functional constraints related to this component lead to develop innovative materials and technologies and refine the simulation of their behaviour which depends on the materials and the manufacturing processes used. The baseline for the european DEMO fusion reactor is to embed divertor actively-cooled plasma facing components made of tungsten as armored material [4]. In DEMO, it is expected that damage will occur in tungsten

[5]. The purpose of this paper is to present a newly developed numerical tool able to assess the tungsten lifetime under DEMO tokamak operation conditions. This tool named T-REX (for Tungsten Response assessment based on EXperimental Data) aims at taking into account the influence of both isolated/combined effects of (i) the thermally activated phenomena (restoration/recrystallization) [6] and (ii) the neutron irradiation [7] on mechanical response of tungsten to assess the component lifetime.

Inherited from the manufacturing process employed, it is known that the tungsten microstructure can change under annealing (thermally activated phenomena) [6, 8]. This is the result of the competition between the restoration and the recrystallization processes for annealed tungsten [9, 10]. At macroscopic scale this competition leads to a tungsten softening (decrease of the material yield stress [11] and an increase of ductility [12]). At initial state (raw material), tungsten in line with the ITER specifications (highly deformed material) presents a linear elastic ideal plastic behaviour whereas after softening the tungsten presents an important kinematic hardening [13, 14] which is sensitive to the strain rate (elastic-viscoplastic behaviour) [12]. Since several years the scientific community aims at developing representative damage assessment

---

tools for plasma facing component. [15, 16, 17] started to take into account the influence of the thermally activated phenomena to better understand the damage process of tungsten under high thermal loads. For that, the decoupled approaches (thermomechanics and metallurgy) assuming an uniform softened tungsten thickness on the upper part of the tungsten block were done, highlighting that softening process promotes the accumulation of plastic strain and leads to a premature cracking. This first approach paved the way to the development of coupled approach giving thus the opportunity to develop numerical tools able to assist the material and/or component design (RXMAT [18]). To do so, RXMAT (Recrystallization (RX) coupled elastic-viscoplastic MATerial model) takes into account the progressive change of tungsten mechanical properties due to tungsten softening under representative high thermal loads. Indeed, the softening implies a decrease of the tungsten mechanical properties which promotes the accumulation of plastic strain that can lead to tungsten failure. From the mechanical point of view, RXMAT [18] assumes an elastic-viscoplastic behaviour for tungsten and softened tungsten and use as input the available tungsten softening kinetics identified at high temperatures [6].

To develop more relevant damage assessment tool, the influence of the neutron irradiation is proposed to be taken into account in the T-REX tool. The energetic neutron (14MeV) produced from the nuclear reaction between the Deuterium (D) and the Tritium (T) will induce defects in the tungsten bulk (cavities, dislocations networks, precipitates) [19]. This will lead to embrittlement (increases of: hardness [16, 19, 20], yield stress [21, 22] and Ductile to Brittle Transition Temperature [23, 24]) and to the degradation of the tungsten thermal properties (highlighted under proton irradiation in [25]) at macroscopic scale. To characterize the thermomechanical properties at relevant operating conditions, the scientific community is waiting for the start of IFMIF-DONES facility to expose tungsten at representative fusion neutron source and spectrum [26, 27]. Up to now, the available data presented in [28] gives a trend regarding the evolution of the tungsten hardness increment up to 2 dpa (displacement per atoms) as a function of the dpa dose (for several tungsten grades from single crystal to stress-relieved and softened tungsten exposed to different neutron sources and spectra). In DEMO, 3 dpa are expected after 2 full power years [29]. The expected dpa rate is 10^{-6} dpa/s [30].

Plasma/wall interactions should also be considered in the modeling. Chemical species presents in the plasma (He, D, T) can diffuse and be trapped in tungsten [31] leading to change locally the mechanical [32] and thermal [33] properties and also the softening kinetics of tungsten [34, 35]. However due to limited data available at macroscopic scale [36], the plasma/wall interactions will be not taking into account in the first phase development of the T-REX tool.

The first part of this paper presents the T-REX tool

(its related assumptions and the constitutive equations). In the second part, parameters needed to take into account the neutron irradiation impact on the mechanical behavior and properties changes are identified based on the data available in literature. In the third part, the influence of the dpa dose, on the mechanical stress and strain fields of the current defined ITER and DEMO tungsten divertor baseline geometries, is studied.

2. The T-REX tool

2.1. Basis and assumptions

The T-REX tool is based on the existing RXMAT tool described in [18]. Historically, RXMAT focuses on the plastic strain assessment. Indeed, the post-mortem experiments highlight the tungsten macro cracking observed after few tens up to few hundreds thermal cycles at 20 MW/m² [39, 40, 41, 42, 43, 44] results of an accumulation of plastic strain near the loaded surface [39]. Plastic strain is a non-reversible deformation of a material at the macroscopic scale. At finer scale (sub grain scale), the plasticity results from the rearrangement or the generation of dislocations which occurs in response to external forces. In low cycle fatigue, the final lifetime (corresponding to the crack opening) is driven by the plastic strain magnitude, which is numerically given by the accumulated equivalent plastic strain increment (Δp) obtained after each thermal cycle. Thus, from the use of low cycle fatigue relationships (known for tungsten and softened tungsten) which relate the plastic strain increment to a number of cycles to failure, it is possible to assess the component lifetime [15, 18].

To better understand the damage process of tungsten component under representative DEMO conditions, T-REX tool proposes to consider, in addition to the softening process, the neutron irradiation in the estimation of Δp to assess the lifetime. **RXMAT inherent assumptions are conserved**. RXMAT is **a parallel elastic-viscoplastic model assuming a linear kinematic hardening** for tungsten and softened tungsten (figure 1). The model solves in parallel the Cauchy stresses and the related state variables in each branch (Tungsten and softened tungsten) assuming an equal total deformation in the two branches. Elastic-viscoplastic parameters used for tungsten and softened tungsten are taken from [18]. **Rules of mixture, involving the softening fraction,** are used to estimate the stress and the plastic strain tensors. The softening fraction is **estimated based on the use of an anisothermal Johnson-Mehl-Avrami-Kolmogorov model [37, 38]**.

According to [22], **it can be assumed that neutron irradiated tungsten presents a linear elastic ideal plastic behaviour. Such mechanical behaviour can be modeled based on the elastic-viscoplastic model assuming unique tangent modulus (E_T) (figure 2)** [18]. Neutron induced macroscopic hardening is taken into
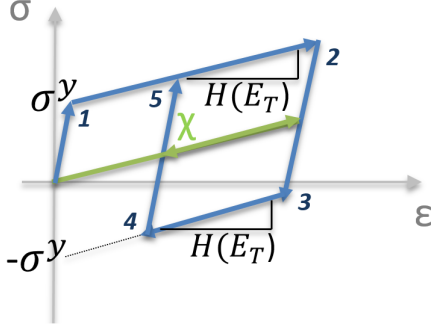
2

Figure 1: Representation of the elastic-viscoplastic mechanical behaviour assumed under cycling loads. With σ^y the yield stress, H the linear plastic slope and E_T the tangent modulus
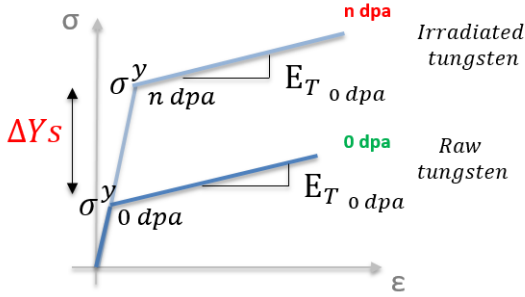

Figure 2: Representation of the elastic-viscoplastic behaviour of tungsten taking into account the neutron irradiation induced hardening under monotonic loading

account. It is assumed that the neutron irradiation leads to the increase of the material yield stress (ΔYs) [21, 22]. In that manner, the only change regarding the initial RX-MAT tool is the modification induced by irradiation of σ^y: the material yield stress (figure 2). Under neutron irradiation, the tungsten damage process is expected to change due to embrittlement. In the literature the most adapted mechanical parameter to assess the component lifetime under combined loading (neutron irradiation and thermal loading under HHF tests) has not been issued yet for the relevant DEMO operating conditions. As a consequence, in this study, we will use Δp dpa as one parameter to evaluate tungsten integrity.

2.2. T-REX constitutive equations

The T-REX constitutive equations assumed for tungsten, irradiated tungsten and softened tungsten are given in the following (modifications of RXMAT related to the neutron irradiation appear in *purple* [18]). During the simulation, the constitutive equations are integrated step by step in time using a fully implicit algorithm.

The total strain tensor is defined as follow:

$$\varepsilon^{tot} - \varepsilon^{th} = \varepsilon = \varepsilon^e + \varepsilon^p \tag{1}$$

Where:
- ε^{tot}, ε^e, ε^p, ε^{th} correspond to the total strain tensor, the elastic strains tensor, the plastic strains tensor and the thermal strains tensor respectively

The common Hooke's law is used to model the elastic behaviour of the material [45]:

$$\boldsymbol{\sigma} = \boldsymbol{C} : \boldsymbol{\varepsilon^e} = \lambda tr(\boldsymbol{\varepsilon^e}).\boldsymbol{I} + 2\mu\boldsymbol{\varepsilon^e} \tag{2}$$

Where:
- $\boldsymbol{C}$ defines the material elasticity tensor (4th order tensor)
- λ and μ correspond to the Lamé coefficients
- $\boldsymbol{I}$ defines the identity matrix

Norton-Hoff type plastic flow rule is used to introduce viscoplasticity:

$$\dot{p} = |\dot{\varepsilon}^p| = < \frac{J(\boldsymbol{\sigma} - \boldsymbol{\chi}) - \sigma^y}{K} >^n \tag{3}$$

With:
- K and n two elastic-viscoplastic parameters
- $\boldsymbol{\chi}$ the kinematic hardening variable
- $\langle \rangle$ which defines the Macauley bracket meaning that:
$\langle x \rangle = \left\{ \begin{array}{ccc} x & if & x > 0 \\ 0 & else & \end{array} \right\}$
- $\boldsymbol{\sigma}$ the material stress tensor
- $\dot{p}$ the accumulated equivalent plastic strain rate
- σ^y the yield stress of the material:

Here, σ^y depends on the initial as-received (or softened) tungsten yield stress (σ_0) and ΔYs, as:

$$\sigma^y = \sigma_0 + \Delta Ys \tag{4}$$

σ_0 is a strain rate and temperature dependent parameter [18]. For the numerical calculation, ΔYs is defined as a constant value over the simulation time (**dpa assumed as constant**). This assumption is taken regarding the expected dpa rate for DEMO ($\sim 10^{-6}$ dpa/s) [30] and the simulated time from seconds (plasma shock) to hours (plasma campaign). For 1h, the order of magnitude of the dpa increase is estimated to be $\sim 10^{-3}$ dpa which is considered to be marginal (at the maximum 10% of variation) for the studied irradiation cases (dpa from 0. 01 to 0.3).

The last equation describes the linear simulated kinematic hardening assumed for tungsten, irradiated tungsten and softened tungsten:

$$\boldsymbol{\chi} = \frac{2}{3}H\boldsymbol{\alpha} \tag{5}$$

Where:
- H is defined based on the material Young modulus (E) and the tangent modulus (E_T) (figure 1):

$$H = \frac{E E_T}{E - E_T} \qquad (6)$$

- α is the internal variable associated with kinematic hardening [45]. Without softening:

$$\alpha = \varepsilon^p \qquad (7)$$

With softening:

$$\dot{\alpha} = \dot{\varepsilon}^p - \frac{\dot{\chi}}{\chi}\alpha \qquad (8)$$

The constitutive equations considered in T-REX are discretized to estimate, at each time step, the set of state variables and the stress tensor. In the case of loading induced plasticity, the state variables related to the viscoplasticity are calculated. Knowing all quantities at each integration point, the residual vector obtained on all the elements is tested. If the obtained residual does not satisfy the convergence criterion, a Newton-Raphson type resolution method is used to iteratively correct the nodal displacements.

3. Determination of model parameter related to neutron irradiation: ΔYs

Neutron irradiation leads to significant tungsten hardness increase (ΔHv) at macroscopic scale [28]. ΔHv increases with the increase of dpa [28], whatever the pure tungsten tested (single crystal, stress-relieved, softened and so on). Based on available data, it is proposed to approximate ΔHv as ΔYs by using the following Tabor's law [46]:

$$\Delta Y_s (MPa) \approx \frac{\Delta Hv}{c} \qquad (9)$$

In literature the Tabor constant (c) is set close to **3** for tungsten [19]. Here, **c is set to 3**. Based on the data presented in [22], ΔYs **is assumed as temperature independent parameter** in this paper.

4. Influence of dpa on tungsten damaging for ITER and DEMO divertor geometries

To study the influence of dpa on tungsten, thermo-mechanical simulations representative of the ITER and DEMO divertor target under high heat flux loading are presented. The upcoming simulations focus on the evolution of Δp estimated after each thermal cycle. To be in line with previous literature studies [15, 18], Δp corresponds to half of the plastic strain increment obtained per cycle ($\Delta p'$): $\Delta p = \Delta p'/2$
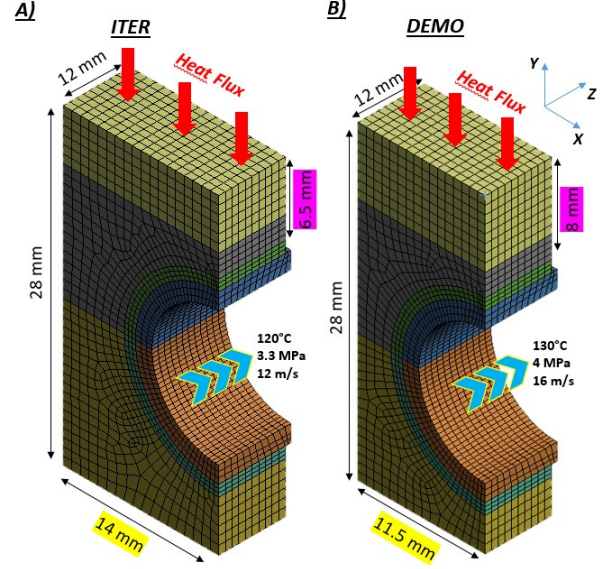

Figure 3: Finite elements models considered for the upcoming simulations assuming either a) the named ITER or b) the named DEMO geometries and meshing for finite elements analysis

4.1. Geometry, meshing, loadings and material properties

Figure 3 presents the two monoblocks geometries representative of the ITER and DEMO divertor targets and their corresponding meshing:

- For ITER, divertor target baseline geometry considers a tungsten blocks (28*28*12mm^3) bonded on a CuCrZr tube ($\phi_{int} = 12\ mm$, $\phi_{out} = 15\ mm$) via a soft cooper interlayer. The minimum thickness of tungsten (distance between the upper surface and the interlayer) is equal to 6.5 mm [15]. This geometry is called later ITER geometry.

- For DEMO, divertor target baseline geometry assumes a tungsten blocks (23*28*12mm^3) bonded on a CuCrZr tube ($\phi_{int} = 12\ mm$, $\phi_{out} = 15\ mm$) via a soft cooper interlayer. The minimum thickness of tungsten is equal to 8 mm [47]. This geometry is called later DEMO geometry.

For these simulations quasi-steady state heat load is assumed. Homogeneous heat flux is cyclically applied on the upper surface (similar to the HHF campaigns). 15 MW/m² and 20 MW/m² as incident heat flux intensities on the upper tungsten surface are taken as simulated cases (figure 3). Thermal cycle is defined as 5 s heating and 5 s cooling. Table 2 gives an overview of the boundary conditions considered for each simulation.

Mechanical responses of copper materials are not studied here. Their mechanical properties are set from data presented in [11].

T-REX is a general elastic-viscoplastic tool. Material properties and other properties used as input can be selected arbitrarily by the user. In this paper, young modulus, heat conductivity and coefficient of thermal expansion

4

used for tungsten, softened tungsten and neutron irradiated tungsten are given in table 1.

For tungsten and neutron irradiated tungsten E_T is set as constant value equal to 0.85 GPa [18]. For softened tungsten, E_T is set to a temperature dependent parameter (table 1). In the upcoming simulations several dpa doses are assumed from 0 to 0.3 dpa.

Table 2 gives an overview of the simulations performed in this paper and highlights the values considered for ΔYs at 0.01, 0.1 and 0.3 dpa. Related ΔYs are estimated based on the data presented in [28] and the equation 9. For the upcoming simulations, raw tungsten is assumed at the initial simulation time (t_0) and softening is neglected (no softening occurs over the thermal cycles) expect for one simulation considering the DEMO geometry (the last simulation presented in table 2) at 0 dpa. The current knowledge of the irradiated tungsten softening kinetics do not allow to make any assumptions about the softening process at higher dpa ($>$0).

4.2. Numerical results and discussions

Figure 4 presents the evolution of Δp in tungsten as function of dpa for the ITER and DEMO geometries under thermal cycling loads at 15 and 20 MW/m². For each simulation, Δp presented is the one obtained during the 5th thermal cycle (stabilized value).

As excepted, it can be seen that Δp decreases with the dpa increase. For the ITER geometry at 20 MW/m², Δp decreases from 0.73% at 0 dpa to 0.06% at 0.3 dpa. As Δp reaches value close to 0 at 0.3 dpa, damage process could be not governed by plasticity above 0.3 dpa.

Figure 4 highlights also the influence of the incident thermal heat flux intensity on the evolution of Δp. Comparing the results obtained for ITER geometry at 20 MW/m² to the ones obtained for the same geometry at 15 MW/m², it can be seen that the Δp is lower for the case of the 15 MW/m² loading case whatever the dpa dose. For this stated geometry, it can also be noted that the damage process should not be governed by plasticity above 0.1 dpa (for the 15 MW/m² loading case).

Figure 4 highlights the influence of the tungsten block geometry on the evolution of Δp. It can be seen that Δp for DEMO geometry is lower than the one obtained for the ITER geometry at a stated heat flux and dpa.

One can be also noted that for this stated DEMO geometry, the damage process should not be governed by plasticity beyond 0.1 dpa whatever the heat flux intensity.

Numerical results obtained for DEMO geometry also revealed that maximum of Δp is obtained on the side face of the monoblock (figure 4). Even if plastic strain accumulation did not lead to macroscopic damage during the recent high heat flux experiments for DEMO relevant components [47, 48], its related damage process have to be further investigated (numerically [49] and experimentally).

Figure 5 shows the evolution of Δp over several thermal cycles at 20 MW/m² for two simulations considering DEMO geometry and taking into account either the softening process or not. Without softening, Δp is constant over the thermal cycles. For the simulations where softening is taken into account, Δp increases due to softening which starts from the fourth thermal cycle. Δp stabilized after the 25th cycles due to fully softened tungsten all around the point A. The increase of Δp promotes the accumulation of plastic strain over the thermal cycle and lead to a premature cracking of the tungsten (as shown in [18]).

With taken assumptions, the first application of the T-REX tool aims at assessing the operating domain (heat flux, dpa) for which the damage is induced by plasticity in tungsten divertor component under homogeneous heat flux. It is shown that the level of damage induced by plasticity depends on the geometry. By geometry optimization, an abatement of Δp can be beneficial for the tungsten lifetime in the case of tungsten damage process governed by plasticity.

Under neutron irradiation, it is highlighted that an abatement of Δp should also occur. However, figure 4 highlights that neutron irradiation can lead to a total disappearance of plastic strain above 0.1 dpa for all numerical cases achieved (excepted for ITER geometry at 20 MW/m²). This results from a strong tungsten embrittlement which could lead to premature tungsten brittle failure. To a certain extent, softening process, which leads to increase tungsten ductility, could be virtuous under neutron irradiation. Recent results presented in [22] highlight that irradiated tungsten softening lead to (partially) restore ductility, resetting thus, part of the induced hardening. This softening phenomena may result to the partial (or total) annihilation of the neutron induced defects (except precipitates) in tungsten [50]. These last aspects should be further investigated (experimentally and numerically).

5. Conclusions

This paper introduces a developed numerical tool (T-REX) able to asses damage in tungsten taking into account the influence of both isolated and combined heat flux/neutron loading on tungsten mechanical properties changes. This lead to improve the estimation of stress and strain mechanical fields. For that, T-REX assumes:

- An elastic-viscoplastic behaviour for tungsten, irradiated tungsten, softened tungsten

- dpa as constant over the simulation time

- dpa leads to a shift of yield stress (independent temperature parameter)

This paper gives also the opportunity to study the influence of the dpa on the evolution of the plastic strain increment estimated per thermal cycle (Δp). Results obtained highlights that, as expected and according to the experiments on irradiated tungsten, for a stated geometry:

Tungsten/Irradiated tungsten (softened tungsten)				
Temperature	20°C	400°C	800°C	1200°C
Thermal conductivity (α, (W/mK)[11]	**173**(=)	**140**(=)	**118**(=)	**105**(=)
Coefficient of thermal expansion (10^{-6}/K)[11]	**397**(=)	**390**(=)	**368**(=)	**356**(=)
Young Modulus (E, (GPa)[11]	**4,50**(=)	**4,63**(=)	**4,81**(=)	**4,98**(=)

$$\sigma^{\mathbf{y}}(\mathbf{Pa}) = \mathbf{-112000 \times T + 608 \times 10^6} \ (\sigma^y = -4743.94 \times T + 7.97 \times 10^6) \ [18]$$
$$\mathbf{K = -526518.72 \times T + 430 \times 10^6} \ (K = -71003.7 \times T + 1.51 \times 10^8)[18]$$
$$\mathbf{n = 0.0035 \times T - 0.027} \ (n = 0.0067 \times T + 2.58)[18]$$
$$\mathbf{E_T(Pa) = 0.85 \times 10^9} \ (E_T = -2947462.7 \times T + 74.63 \times 10^8)[18]$$

Table 1: Thermal and mechanical properties considered for tungsten, irradiated tungsten and softened tungsten

Geometry	Material at t_0	Convection (°C / MPa / m/s)	$\Delta Ys/dpa$ (MPa/dpa)	flux intensity (MW/m²)
ITER	Raw tungsten (no softening)	120 / 3.3 / 12	0/0	15
				20
			100/0.01	15
				20
			400/0.1	15
				20
			733/0.3	15
				20
DEMO	Raw tungsten (no softening)	130 /4 /16	0/0	15
				20
			100/0.01	15
				20
			400/0.1	15
				20
			733/0.3	15
				20
DEMO	Raw tungsten (with softening)	130 /4 /16	0/0	20

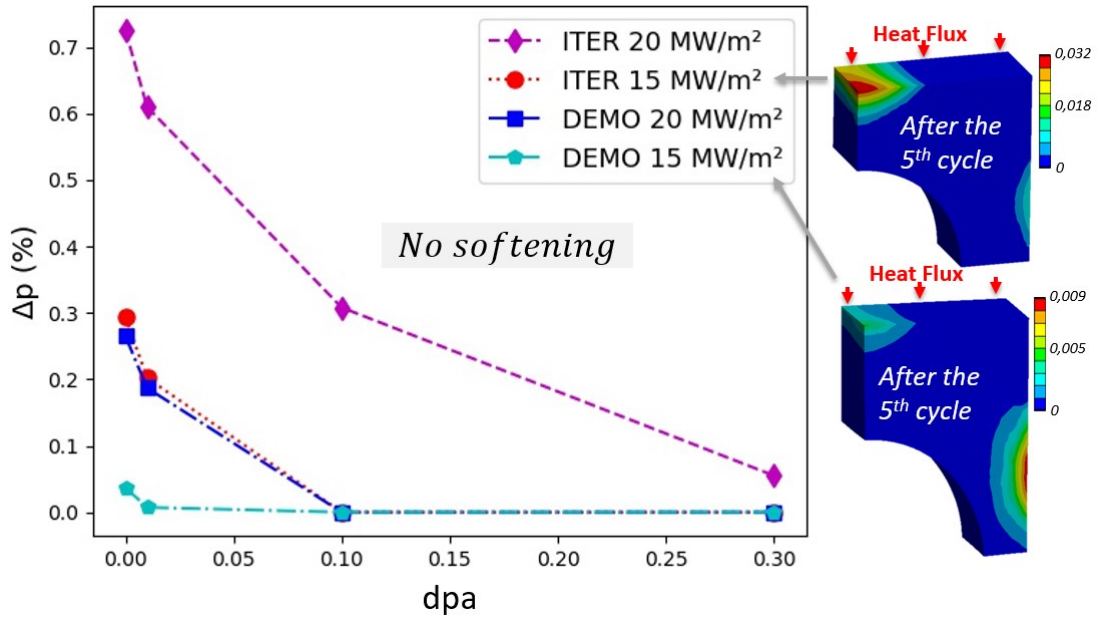Table 2: Overview of the performed simulations

Figure 4: Equivalent plastic strain increment (Δp) obtained as function of the dpa dose for ITER and DEMO geometries under thermal cycles at 15 MW/m² and 20 MW/m² (dashed lines are only given for guiding eyes). Δp are those obtained during the 5th thermal cycle (softening neglected). On the right side, accumulated equivalent plastic strain gradients are also displayed.
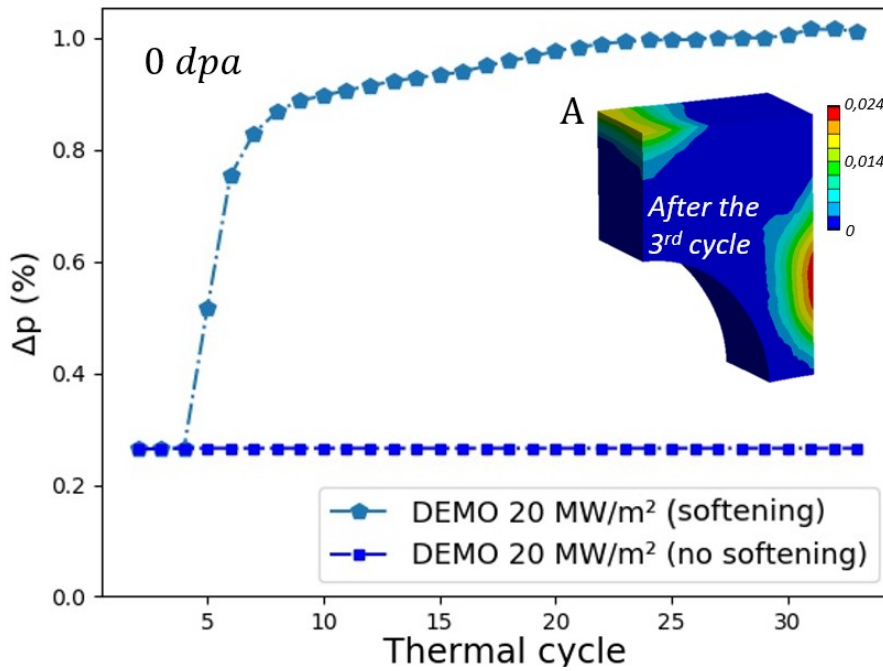

Figure 5: Influence of tungsten softening on Δp at point A (dashed lines are only given for guiding eyes)

- and for a stated heat flux, Δp decreases with the dpa

- and for a stated dpa, Δp increases with the flux intensity

With taken assumptions, the tool provides the assessment of the operating domain (heat flux, dpa) for which the damage is induced by plasticity. With the study performed on ITER and DEMO divertor target geometries, it is shown that the geometry may be optimized to reduce the damage induced by plasticity.

Finally, open questions lead to several perspectives. As short terms one, T-REX project plans to study the influence of softening induced by annealing on the regeneration of Δp for neutron irradiated tungsten.

6. Acknowledgments

DEMO, tungsten, modeling, lifetime, damage, softening, irradiation, neutron

––––––––––––––––

References

[1] A. Grosman et al, The WEST programme: Minimizing technology and operational risks of a full actively cooled tungsten divertor on ITER, Fusion Engineering and Design 88 (2013) 497– 500 https://doi.org/10.1016/j.fusengdes.2013.02.039

[2] G. Frederici et al, European DEMO design strategy and consequences for materials, Nucl. Fusion 57 (2017) 092002 (26pp) https://doi.org/10.1088/1741-4326/57/9/092002

[3] R.A. Pitts et al, A full tungsten divertor for ITER: Physics issues and design status, Journal of Nuclear Materials Volume 438, Supplement, July 2013, Pages S48-S56, https://doi.org/10.1016/j.jnucmat.2013.01.008

[4] J.H. You et al, Progress in the initial design activities for the European DEMOdivertor: Subproject "Cassette", Fusion Engineering and Design 124 (2017) 364–370, http://dx.doi.org/10.1016/j.fusengdes.2017.03.018

[5] M. Diez et al, In situ observation of tungsten plasma-facing components after the first phase of operation of the WEST tokamak, Nucl. Fusion 61 106011, https://doi.org/10.1088/1741-4326/ac1dc6

[6] M. Richou et al, Recrystallization at high temperature of two tungsten materials complying with the ITER specifications, Journal of Nuclear Materials 542 (2020) 152418, https://doi.org/10.1016/j.jnucmat.2020.152418

[7] R.G. Abernethy (2017) Predicting the performance of tungsten in a fusion environment: a literature review, Materials Science and Technology, 33:4, 388-399, https://doi.org/10.1080/02670836.2016.1185260

[8] V. Shah et al, Experimental investigation of the microstructural changes of tungsten monoblocks exposed to pulsed high heat loads, Nuclear Materials and Energy 22 (2020) 100716, https://doi.org/10.1016/j.nme.2019.100716

[9] A. Alfonso et al, Recrystallization kinetics of warm-rolled tungsten in the temperature range 1150–1350 C, Journal of Nuclear Materials 455 (2014) 591–594, http://dx.doi.org/10.1016/j.jnucmat.2014.08.037

[10] L. Karanja et al, An Attempt to Assess Recovery/Recrystallization Kinetics in Tungsten at High Temperature Using Statistical Nanoindentation Analysis, Crystals 2021, 11(1), 37, https://doi.org/10.3390/cryst11010037

[11] ITER Structural design criteria for in-vessel components (SDC-IC) appendix A: Materials design limit data , g74ma, 8 01-05-28w0.2, 2013

[12] A.Durif et al, Impact of tungsten recrystallization on ITER-Like components for lifetime estimation, Fusion Engineering and Design 138 (2019) 247-253, https://doi.org/10.1016/j.fusengdes.2018.11.003

[13] W.Bahm. Nuclear fusion programme annual report of the assiociation Forschungszentrum Karlsruhe / euratom, January 2004 - December 2004. Technical report. 31.00.00; LK 01; Wissenschaftliche Berichte, FZKA-7117 (May 2005) EUR-21526-EN

[14] J. Habainy et al, Fatigue behavior of rolled and forged tungsten at 25, 280 and 480 C, Journal of Nuclear Materials 465 (2015) 438e447, http://dx.doi.org/10.1016/j.jnucmat.2015.06.032

[15] M. Li and J.-H. You, "Interpretation of the deep cracking phenomenon of tungsten monoblock targets observed in high-heat-flux fatigue tests at 20 MW/m2," Fusion Eng. Des., vol. 101, pp. 1–8, Dec. 2015, http://dx.doi.org/10.1016/j.fusengdes.2015.09.008

[16] S. Nogami et al, Degradation of tungsten monoblock divertor under cyclic high heat flux loading, Fusion Engineering and Design 120 (2017) 49–60, http://dx.doi.org/10.1016/j.fusengdes.2017.04.102

[17] M. Furdson et al, Towards reliable design-by-analysis for divertor plasma facing components – Guidelines for inelastic assessment (part 1: Unirradiated), Fusion Engineering and Design 147 (2019) 111234, https://doi.org/10.1016/j.fusengdes.2019.06.007

[18] A. Durif et al, Numerical study of the influence of tungsten recrystallization on the divertor component lifetime, International Journal of Fracture volume 230, pages83–98 (2021), https://doi.org/10.1007/s10704-021-00568-1

[19] X. Hu et al, Irradiation hardening of pure tungsten exposed to neutron irradiation, Journal of Nuclear Materials 480 (2016) 235e243, http://dx.doi.org/10.1016/j.jnucmat.2016.08.024

[20] D. Terentyev et al, Neutron irradiation hardening across ITER diverter tungsten armor, International Journal of Refractory Metals and Hard Materials Volume 95, February 2021, 105437, https://doi.org/10.1016/j.ijrmhm.2020.105437

[21] T. Miyazawa et al, Neutron irradiation effects on the mechanical properties of powder metallurgical processed tungsten alloys, Journal of Nuclear Materials Volume 529, February 2020, 151910, https://doi.org/10.1016/j.jnucmat.2019.151910

[22] T. Miyazawa et al, Tensile properties of powder-metallurgical-processed tungsten alloys after neutron irradiation near recrystallization temperatures, Journal of Nuclear Materials 542 (2020) 152505, https://doi.org/10.1016/j.jnucmat.2020.152505

[23] R.G. Abernethy et al, Effects of neutron irradiation on the brittle to ductile transition in single crystal tungsten, Journal of Nuclear Materials 527 (2019) 151799, https://doi.org/10.1016/j.jnucmat.2019.151799

[24] E. Gaganidze et al, Fracture-mechanical properties of neutron irradiated ITER specification tungsten, Journal of Nuclear Materials Volume 547, 15 April 2021, 152761, https://doi.org/10.1016/j.jnucmat.2020.152761

[25] J. Habainy et al, Thermal diffusivity of tungsten irradiated with protons up to 5.8 dpa, Journal of Nuclear Materials 509 (2018) 152e157, https://doi.org/10.1016/j.jnucmat.2018.06.041

[26] S.M. Gonzalez De Vicente, Materials testing facilities and pro-

grammes for fission and ion implantation damage, Nucl. Fusion 57 092011, https://doi.org/10.1088/1741-4326/aa6a67

[27] D. Stork et al, Towards a programme of testing and qualification for structural and plasma-facing materials in 'fusion neutron' environments, Nucl. Fusion 57, https://doi.org/10.1088/1741-4326/aa60af

[28] S. Nogami et al, Mechanical properties of tungsten: Recent research on modified tungsten materials in Japan, Journal of Nuclear Materials 543 (2021) 152506, https://doi.org/10.1016/j.jnucmat.2020.152506

[29] S. Noce et al, Nuclear analyses for the design of the ITER-like plasma facing components vertical targets of the DEMO divertor, Fusion Engineering and Design 155 (2020) 111730, https://doi.org/10.1016/j.fusengdes.2020.111730

[30] S. Ishino et al, Need for and Requirements for a Neutron Irradiation Facility for Fusion Materials Testing, Journal of Fusion Energy, Vol. 8, Nos. 3/4, 1989

[31] M. Miyamoto et al, Microscopic damage of tungsten exposed to deuterium–helium mixture plasma in PISCES and its impacts on retention property, Journal of Nuclear Materials 415 (2011) S657–S660, https://doi:10.1016/j.jnucmat.2011.01.008

[32] A. Hasegawa et al, Helium effects on recovery and recrystallization of powder metallurgically processed tungsten, Phys. Scr. T171 (2020) 014016 (7pp), https://doi.org/10.1088/1402-4896/ab408d

[33] S. Cui et al, Thermal conductivity reduction of tungsten plasma facing material due to helium plasma irradiation in PISCES using the improved 3-omega method, Journal of Nuclear Materials 486 (2017) 267e273, http://dx.doi.org/10.1016/j.jnucmat.2017.01.023

[34] K. Song et al, Temperature dependence of retarded recrystallisation in helium plasma-exposed tungsten, Nucl. Fusion 59 (2019) 096031 (10pp) https://doi.org/10.1088/1741-4326/ab2e3c

[35] Wangguo Guo et al, Retarded recrystallization of helium-exposed tungsten, Fusion 58 (2018) 106011 (8pp), https://doi.org/10.1088/1741-4326/aad2b0

[36] K. Sato et al, Investigation of mechanical properties of stress-relieved and electron irradiated tungsten after hydrogen charging, Nuclear Materials and Energy 17 (2018) 29–33, https://doi.org/10.1016/j.nme.2018.08.003

[37] J-M.Bergheau (2014),Thermomechanical Industrial Processes: Modeling and Numerical Simulation. ISTE. Wiley

[38] A. Durif et al, Inverse identification of tungsten static recrystallization kinetics under high thermal flux, Fusion Engineering and Design 146 (2019) 1759–1763, https://doi.org/10.1016/j.fusengdes.2019.02.141

[39] G. Pintsuk et al., Characterization of ITER tungsten qualification mock-ups exposed to high cyclic thermal loads, Fusion Eng. Des., vol. 9899, pp. 13841388, Oct. 2015, http://dx.doi.org/10.1016/j.fusengdes.2015.01.037

[40] G. Pintsuk et al, High heat flux testing of newly developed tungsten components for WEST, Fusion Engineering and Design 173 (2021) 112835, https://doi.org/10.1016/j.fusengdes.2021.112835

[41] K. Ezato et al., Progress of ITER full tungsten divertor technology qualification in Japan, Fusion Eng. Des., vol. 98–99, pp. 1281–1284, Oct. 2015, http://dx.doi.org/10.1016/j.fusengdes.2015.03.009

[42] P. Gavila et al., High heat flux testing of mock-ups for a full tungsten ITER divertor, Fusion Eng. Des., vol. 86, no. 9–11, pp. 1652–1655, Oct. 2011, http://dx.doi.org/10.1016/j.fusengdes.2014.12.006

[43] G.Pintsuk et al, Qualification and post-mortem chracterization of tungsten mock-ups exposed to cyclic high heat flux loading, Fusion Engineering and Design 88 (2013), 1858-1861, http://dx.doi.org/10.1016/j.fusengdes.2013.05.091

[44] S. Panayotis et al, Self-castellation of tungsten monoblock under high heat flux loading and impact of material properties, Nuclear Materials and Energy 12 (2017) 200–204

[45] J.Lemaitre and J.Chaboche (2004). Mécanique des matrériaux solides. Sciences SUP. Science de l'ingénieur. Dunod.

[46] Tabor D., The hardness of metals, 1951 , Oxford Claredon press, Oxford

[47] J-H. You et al, High-heat-flux technologies for the European demo divertor targets: State-of-the-art and a review of the latest testing campaign, Journal of Nuclear Materials 544 (2021) 152670, https://doi.org/10.1016/j.jnucmat.2020.152670

[48] H. Greuner et al, Assessment of the high heat flux performance of European DEMO divertor mock-ups, Phys. Scr. T171 (2020) 014003 (7pp), https://doi.org/10.1088/1402-4896/ab3681

[49] J-H. You et al, Structural lifetime assessment for the DEMO divertor targets: Design-by-analysis approach and outstanding issues, Fusion Engineering and Design 164 (2021) 112203, https://doi.org/10.1016/j.fusengdes.2020.112203

[50] A. Mannheim et al, Controlled irradiation hardening of tungsten by cyclic recrystallization, Modelling Simul. Mater. Sci. Eng. 27 (2019) 065001 (28pp), https://doi.org/10.1088/1361-651X/ab1eec